Postoperative metastatic Krukenberg tumors with *ARID1A* and *KRAS* mutations in a patient with gastric cancer treated with oxaliplatin and tegafur: A case report

JIE WU[1], SUZHEN JIANG[1], QINGLING SHEN[1] and HONGXIA GONG[2]

[1]Department of Gynecology, Dongguan Songshan Lake Tungwah Hospital, Dongguan, Guangdong 523000, P.R. China; [2]Department of Gynecology, Dongguan Tungwah Hospital, Dongguan, Guangdong 523000, P.R. China

Received October 13, 2024; Accepted March 14, 2025

DOI: 10.3892/ol.2025.15008

Abstract. Krukenberg tumors are a notably rare type of metastatic ovarian malignant tumor, often originating from the stomach. Due to their low incidence rate and the short survival time of patients, there is currently a lack of consensus on the diagnosis and treatment of this disease, as well as a deficiency in genomic analyses and research into the pathogenetic molecular mechanisms. In the present study, the case of a patient with gastric cancer who, 2 years after curative surgery and chemotherapy with oxaliplatin and tegafur, developed recurrent metastatic bilateral Krukenberg tumors with distant metastasis in the ovaries. During treatment, a total hysterectomy and bilateral salpingo-oophorectomy were performed, and intraoperative intraperitoneal chemotherapy with cisplatin (70 mg) was administered. Additionally, ureteroscopy and bilateral ureteral stent placement were conducted transurethrally. Post-surgery, assessments of the genomic alterations and microsatellite instability of the tumor revealed an AT-rich interaction domain 1A (*ARID1A*) exon c.4720delC mutation and a *KRAS* exon c.35G>C mutation. The potential pathogenic mechanisms and clinical significance of these mutations were then further discussed. Mutations in the *ARID1A* gene could increase the sensitivity of the patient to immune checkpoint inhibitor therapy. Additionally, the successful application of $KRAS^{G12C}$ inhibitors in other cancer types offers a new approach for the targeted therapy of Krukenberg tumors. Therefore, the present study provides further evidence regarding the genomics of Krukenberg tumors, which may aid in the development of targeted treatment strategies.

Correspondence to: Dr Hongxia Gong, Department of Gynecology, Dongguan Tungwah Hospital, 1 Dongcheng East Road, Dongcheng, Dongguan, Guangdong 523000, P.R. China
E-mail: 13538634373@163.com

Key words: Krukenberg tumor, metastatic ovarian cancer, next-generation sequencing, AT-rich interaction domain 1A, *KRAS*, mutation

Introduction

Globally, ovarian cancer is a primary cause of cancer-related death among women with malignant tumors of the reproductive system (1). Krukenberg tumors, a specialized form of metastatic ovarian cancer, are histologically defined by the presence of mucin-filled signet ring cells (2). Predominantly, these tumors originate from the stomach (76%), with the colorectum being the next most common primary site (11%), classifying them as rare and highly malignant metastatic neoplasms with a poor patient prognosis (2-4). The rarity of Krukenberg tumors, coupled with the typically short survival time of those affected, results in a lack of consensus regarding their diagnosis and treatment (3,5). Furthermore, the absence of comprehensive genomic data impedes research into the underlying molecular mechanisms of this disease (6). These factors constrain the comprehension of this rare disease and impede the advancement of targeted treatment strategies.

The present study focused on two critical oncogenes: AT-rich interaction domain 1A (*ARID1A*) and *KRAS*. The *KRAS* gene is commonly mutated in multiple types of cancer, including pancreatic cancer, colorectal cancer (CRC) and lung adenocarcinoma (7-9). *KRAS* encodes a protein that is a key component of the MAPK/ERK signaling pathway (10), which serves a notable role in cell proliferation, differentiation and survival (11). Mutations in *KRAS* typically lead to the constitutive activation of this pathway, promoting the continuous proliferation of tumor cells, and are associated with tumor aggressiveness and therapeutic resistance (12). The *ARID1A* gene is an N-terminal acetyltransferase (13), and its function is closely related to the occurrence, progression and metastasis of various types of cancer, including ovarian cancer, endometrial cancer and gastric cancer (GC) (14-17). *ARID1A* regulates the activity of cyclin proteins by inactivating β-catenin, thereby affecting the progression of the cell cycle (18). Moreover, mutations in *ARID1A* are also associated with alterations in the tumor immune microenvironment, potentially enhancing the sensitivity of tumors to immunotherapy by affecting the stimulator of interferon (IFN) genes (STING)/IFN signaling pathway and promoting a robust antitumor T-cell response (14,19,20).

The present report describes the case a patient who underwent adjuvant chemotherapy with oxaliplatin and tegafur

following curative resection for GC. The present study aims to provide further genomics research into Krukenberg tumors, but also to provide novel insights into understanding the pathogenesis of Krukenberg tumors and exploring personalized treatment strategies.

Case report

In September 2023, a 46-year-old female patient was admitted to the Department of Obstetrics and Gynecology, Dongguan Songshan Lake Tungwah Hospital (Dongguan, China), presenting with abdominal distension and difficulty urinating. The patient had experienced progressively worsening abdominal distension within 2 months and had lost 3 kg in weight within the 2 weeks prior to admission. The patient had undergone curative surgery for GC in July 2021, with the pathological results indicating poorly differentiated adenocarcinoma of the stomach, with some areas presenting characteristic signet ring cells. Postoperatively, the patient received chemotherapy with oxaliplatin (150 mg, intravenous) and tegafur (160 mg, oral) for eight cycles. The patient denied experiencing any abnormal vaginal bleeding. On physical examination in September 2023, a 10-cm diameter ovarian mass was palpated behind and to the right of the uterus, which was hard in texture, poorly mobile and non-tender. The laboratory tests revealed CA199 at 96.0 U/ml (normal range 0-30 U/ml), CEA at 1.66 ng/ml (normal range 0-5 ng/ml), CA125 at 33.4 U/ml (normal range 0-47 U/ml), human epididymis protein 4 at 420.6 pmol/l (normal range 0-76.2 pmol/l) and AFP at 2.6 IU/ml (normal range 0-7 IU/ml). Both CA199 and human epididymis protein 4 were above the normal levels; hemoglobin was 54 g/l (normal range 115-155 g/l) and creatinine was 135.2 μmol/l (normal range 44-97 μmol/l).

An abdominal color Doppler ultrasound indicated a hypoechoic mass behind the uterus, measuring ~110x67x47 mm, with imaging revealing abundant blood flow signals within the mass (Fig. 1A and B). Enhanced abdominal computed tomography (CT) clearly depicted the tumor vasculature and necrotic lesions. An irregular cystic-solid mass was observed in the pelvic cavity, which began to enhance earlier than the uterine wall after the injection of contrast medium Ioversol, showing heterogeneous hyperenhancement. A large vessel could be observed entering the mass from one side, and heterogeneous enhancement areas within the mass were noted, which are indicative of tumor necrosis or liquefaction, signs suggestive of a malignant tumor (Fig. 1C-F). Due to the accompanying symptoms of difficulty urinating, further examination with CT urography and three-dimensional reconstruction revealed an irregular mass in the pelvic cavity, with compression and narrowing of the lower segments of both ureters, leading to dilatation of the upper ureteral segments and bilateral hydronephrosis. There was a notable delay in the excretion of the right urinary system, with local suspected obstruction, surrounding exudate and possible tumor invasion requiring further investigation (Fig. 1G and H).

The patient was informed that the treatment options included chemotherapy or cytoreductive surgery. The following treatment plan was determined based on the preference of the patient: Total abdominal hysterectomy, bilateral salpingo-oophorectomy, pelvic adhesiolysis, transurethral bilateral ureteroscopy and bilateral ureteral stent placement. The patient initially underwent a challenging surgical procedure with thorough exploration of the pelvic and abdominal cavities, the observations included: ~100 ml mucinous ascites in the pelvic and abdominal cavities, as well as two solid masses behind the uterus, originating from the ovaries, measuring ~70x50x40 mm on the left and 50x40x30 mm on the right. The surfaces of the masses were smooth with intact capsules, exhibiting a reniform shape. The rest of the abdomen and organ surfaces were smooth with no obvious lesions. The bilateral adnexa and masses were resected (Fig. 2A-C). Frozen section diagnosis revealed poorly differentiated carcinoma of the ovaries on both sides, with some cancer cells exhibiting signet ring cell carcinoma (SRCC), consistent with metastatic GC. Consequently, an additional total hysterectomy was performed and transurethral ureteroscopy plus bilateral ureteral stent placement was conducted intraoperatively. The surgical exploration revealed pale mucosa of the bilateral ureters, with the middle and upper segments becoming narrow and rigid due to compression, and no obvious tumor invasion was seen on the ureteral wall. At the end of the surgery, a single intraperitoneal chemotherapy dose of cisplatin was administered (70 mg in 1,000 ml distilled water).

Postoperatively, further pathological histological examination was conducted. Tissue samples were fixed in 10% neutral-buffered formalin at room temperature for 24 h and embedded in paraffin. Sections 4-μm thick were prepared and stained with hematoxylin for 5 min and eosin for 2 min at room temperature (Fig. 3A-C). The stained sections were examined under a light microscope to identify infiltrating tumor cells in the stroma. Mucin-laden signet ring cells with eccentric hyperchromatic nuclei were observed. These cells were morphologically compatible with the cells of the previously resected gastric adenocarcinoma tissue.

For immunohistochemical analysis, formalin-fixed, paraffin-embedded tissue sections (4 μm) were used. Antigen retrieval was performed by heating at 95˚C in citrate buffer (pH 6.0) for 20 min, followed by washing with xylene and rehydration through a graded ethanol series. Endogenous peroxidase activity was blocked using 3% hydrogen peroxide for 10 min at room temperature. Sections were then incubated with primary antibodies at 4˚C overnight, followed by incubation with HRP-conjugated secondary antibodies for 30 min at room temperature. Immunoreactivity was detected using DAB chromogen, and counterstaining was performed with hematoxylin. The slides were examined under a light microscope. In the immunohistochemical diagnosis, the following markers were positive: Cytokeratin (CK)7, mutL homolog (MLH)1, MLH2, PMS1 homolog 2 and mutS homolog 6, whereas p53 was wild-type and there was no amplification of paired box 8 (PAX8), SATB homeobox 2 (SATB2) or HER-2 (Fig. 3D-L). Based on the pathological results, it was confirmed that the ovarian masses were metastatic carcinoma from the previously treated GC, and the mucin-laden signet ring cells confirmed the diagnosis of Krukenberg tumors.

In September 2023, to identify personalized treatment strategies, whole exome sequencing was performed on ovarian tumor tissue by Letu Biotechnology Co., Ltd. DNA was extracted using the QIAamp DNA Mini Kit (Qiagen, Inc.). Library preparation was conducted using the Agilent SureSelect XT

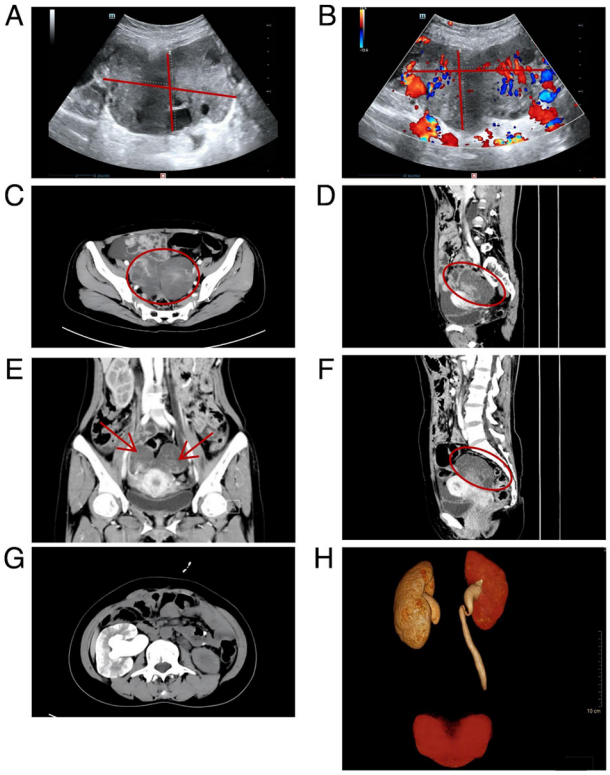

Figure 1. Ultrasound, CT, CTU and three-dimensional reconstruction imaging findings. (A) Ultrasound performed in September 2023 showed a 108x65 mm mass lesion thought to originate from the ovaries that had no clear relationship with the uterus. (B) Color Doppler flow imaging showed markedly increased flow signals bright in the lesion. (C) Enhanced abdominal CT imaging showed a hyperdense mass lesion of 110x67x47 mm, which had a cystic-solid component. (D-F) The lesion was visualized using contrast-enhanced CT: (D) Left and (F) right sagittal views, and (E) coronal view. (G) Multi-slice spiral CTU and intravenous pyelogram imaging showed right renal pelvis dilatation and ureteral stenosis. (H) Right ureteral obstruction was not visible on the CT urography. CT, computed tomography; CTU, CT urography.

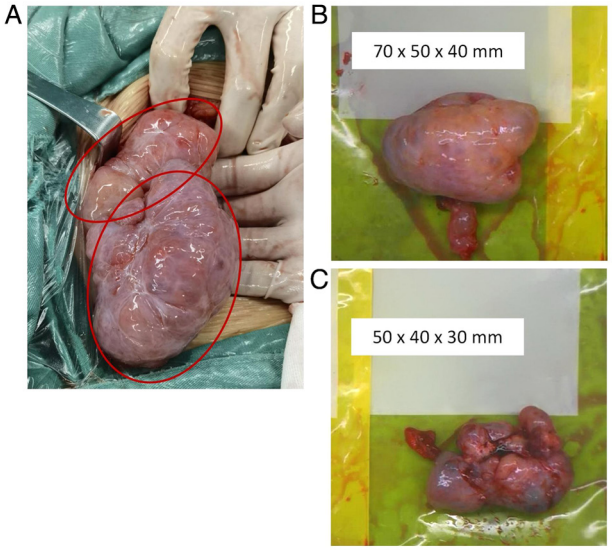

Figure 2. Fresh gross images of the resected tissues. (A) Laparotomy revealed that the tissue was not monolithic and originated from both ovaries. Incision of the tumor revealed a solid cyst profile and clear mucus outflow. (B) The mass on the right ovary measured 50x40x30 mm in size. (C) The mass on the left ovary measured 70x50x40 mm in size.

Human All Exon V8 Kit (Agilent Technologies, Inc.) following the manufacturer's instructions. Sequencing was performed on an Illumina NovaSeq 6000 platform using a paired-end 150 bp strategy. The final library was loaded at a concentration of 10 nM, measured using a Qubit 4 Fluorometer (Thermo Fisher Scientific, Inc.). Genomic DNA was extracted using the FFPE Tissue Genomic DNA One-Step Extraction Kit (Hangzhou Simgen Biotechnology Co., Ltd.) and the QIAamp Circulating Nucleic Acid Kit (Qiagen, Inc.). The xGen Lockdown Probe (Integrated DNA Technologies, Inc.), customized with the KAPA Hyper Prep Kit (Kapa Biosystems; Roche Diagnostics), was used for capture reactions, which were conducted with Dynabeads M-270 (Thermo Fisher Scientific, Inc.) and the xGen Lockdown Hybridization and Wash Kit (Integrated DNA Technologies, Inc.). The libraries were amplified with Illumina p5 and p7 primers using the KAPA HiFi HotStart ReadyMix (Kapa Biosystems; Roche Diagnostics), and the library fragment sizes were determined using the KAPA Library Quantification Kit (Kapa Biosystems; Roche Diagnostics) and a Bioanalyzer 2100 (Agilent Technologies, Inc.). Target-enriched libraries were sequenced on the HiSeq4000 NGS platform (Illumina, Inc.). Data analysis included quality control with Trimmomatic (version 0.39; http://github.com/usadellab/Trimmomatic), alignment with BWA (version 0.7.17; http://github.com/lh3/bwa), PCR duplicate removal with Picard (version 2.23.8; http://github.com/broadinstitute/picard) and variant calling with Mutect2 [version 1.1.7 (legacy) or part of the GATK 4.x series (current); https://gatk.broadinstitute.org/hc/en-us/articles/360037593851-Mutect2] and Scalpel (version 0.5.3; http://github.com/sleuthkit/scalpel). Annotations were performed with vcf2maf (version 1.6.19; http://github.com/mskcc/vcf2maf). The sequencing depth for the tumor tissue control sample was 1,500x.

The DNA sequencing results revealed two genetic mutations (Table I). The *ARID1A* gene harbored a frameshift mutation (c.4720delC), where a cytosine was deleted at the 4,720th position of the DNA sequence, resulting in the change of proline to histidine at the 1,575th amino acid position of the corresponding protein sequence. Additionally, a missense mutation (c.35G>C) was detected in the *KRAS* gene, with a guanine being replaced by a cytosine at the 35th position of the DNA sequence, leading to the change of the 12th amino acid from glycine to alanine in the protein sequence. No abnormalities in terms of gene fusions or copy number variations were observed, and no mutations were found in genes related to the homologous recombinational repair pathway. Microsatellite instability (MSI) indicated a stable microsatellite phenotype.

Postoperatively, the creatinine level of the patient decreased from 135.2 μmol/l (normal range 44-97 μmol/l) preoperatively to 66.0 μmol/l on day 4 after surgery, indicating the restoration of normal kidney function. Given the stage IV (International Federation of Gynecology and Obstetrics, 2021) (21) poorly differentiated adenocarcinoma, adjuvant systemic chemotherapy was recommended. However, the patient, considering their predicted survival rate and financial capacity, chose to decline chemotherapy. Finally, the patient succumbed to the disease in January 2024. The overall survival (OS) time, from the initial diagnosis of GC in July 2021 to the time of death,

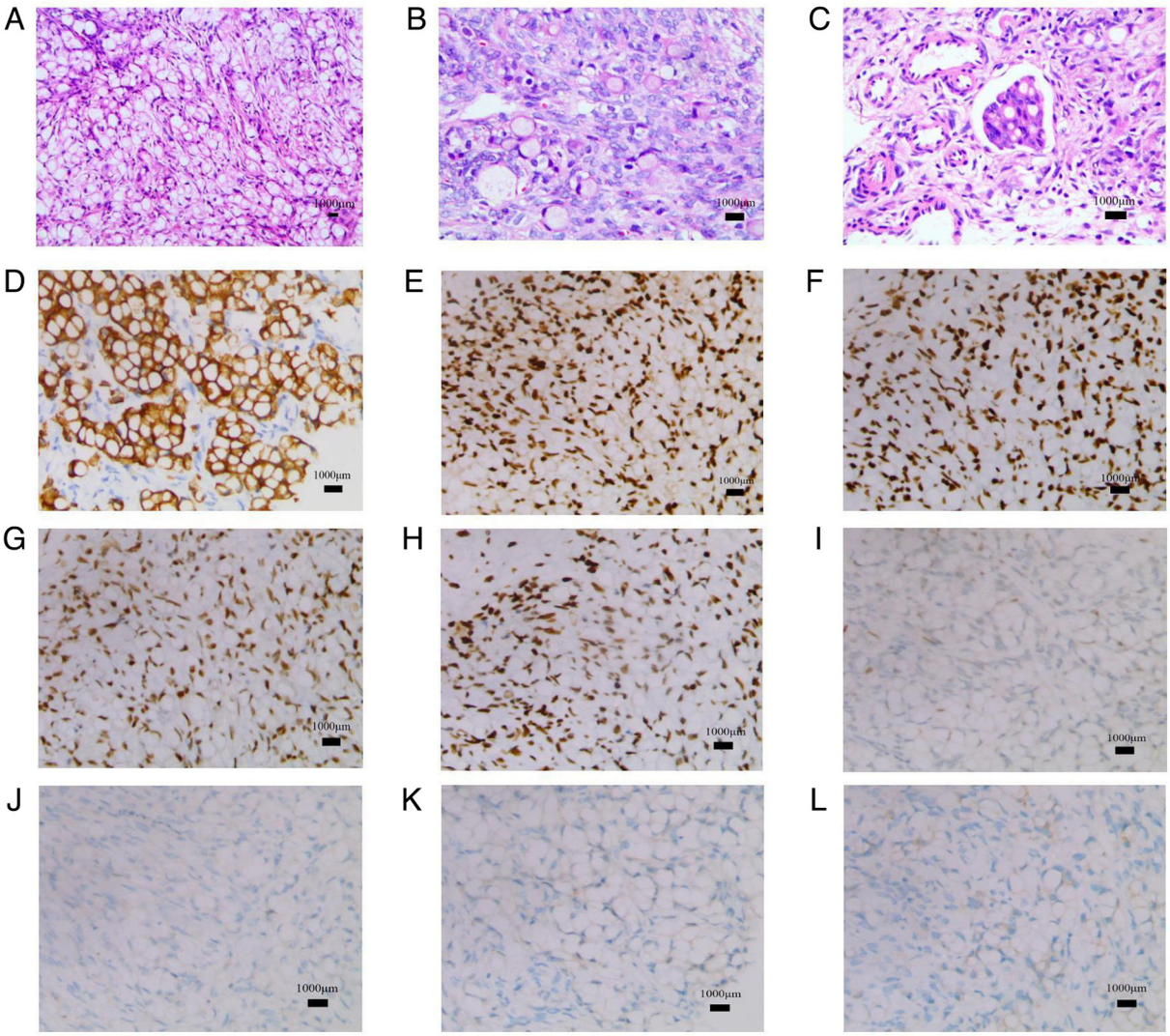

Figure 3. Histological and immunohistochemical findings. (A) Hematoxylin and eosin staining demonstrated the overall morphology of the tissue (magnification, x10). (B and C) Microscopic hematoxylin and eosin findings showed a signet-ring cell carcinoma composed of poorly cohesive tumor cells with abundant intracytoplasmic mucin and eccentric nuclei (magnification, x20). (D) Immunohistochemical staining for cytokeratin 7 highlighted epithelial cells (magnification, x20). (E) Immunohistochemical staining for MLH1, a marker to determine the mismatch repair status (magnification, x20). Immunohistochemical staining for (F) MLH2 (magnification, x20), (G) PMS1 homolog 2 (magnification, x20), (H) mutS homolog 6 (magnification, 20), (I) p53 (magnification, x20), (J) paired box 8 (magnification, x20), (K) SATB homeobox 2 (magnification, x20) and (L) HER-2 (magnification, x20). MLH, mutL homolog.

totaled 30 months. Specifically, the survival period following recurrence with distant metastatic Krukenberg tumors, identified in September 2023, was 4 months.

Discussion

Ovarian metastatic tumors result from the spread of a primary cancer from another site to the ovaries (22), accounting for 10-25% of all ovarian malignancies (23). Krukenberg tumors, as a rare and distinct type of malignant tumor, represent only 1-2% of these metastatic tumors (23,24). Krukenberg tumors are diagnosed at a markedly younger age compared with epithelial ovarian cancer, predominantly affecting premenopausal women with an average age of diagnosis of 45 years (3). A previous retrospective analysis of Krukenberg tumors revealed that the median age at diagnosis for these patients was 48 years, with ages ranging between 22 and 71 years (25). The patient reported in the present study was diagnosed at 46 years old, which is in accordance with the age distribution cited in the literature. Unlike tumors with overt mucin-laden signet ring cells in the pathological histology, the clinical presentation of this type of lesion is often more subtle, manifesting as an abdominal mass with abdominal distension and insidious abdominal pain. Due to its covert onset and lack of distinctive clinical features, when ascites is present, the disease is typically at an advanced stage (23,26). In the present case, the clinical symptoms were limited to a 2-month history of abdominal distension, and physical examination revealed only pelvic masses and dullness to percussion, indicative of ascites.

Preoperative imaging reports also provide a certain reference for the diagnosis of ovarian metastatic tumors. In the present case report, imaging examinations confirmed no notable lesions in other areas besides the adnexal region. Ultrasound indicated a mass behind the uterus with abundant blood flow signals, and enhanced CT suggested that the mass was a complex cystic-solid lesion with irregular shape and heterogeneous enhancement.

Table I. Genome location of single nucleotide variants, and insertion-deletions in tumor tissue.

Gene	Transcript number	Exon	Base change	Amino acid change
ARID1A	NM_006015	Exon 18	c.4720delC	p.P1575Hfs*37
KRAS	NM_004985	Exon 2	c.35G>C	p.G12A

ARID1A, AT-rich interaction domain 1A.

Metastatic ovarian tumors typically manifest as solid or mixed cystic-solid masses, often bilateral and multiple (26), whereas primary ovarian tumors typically present as cystic masses or masses with areas of liquefied necrosis, often unilateral (27,28). In the present case, the imaging results revealed a solitary complex cystic-solid mass with significant enhancement areas, considered to be areas of tumor necrosis or liquefaction, which is different from the presentation of primary ovarian cancer, increasing the difficulty of diagnosis.

The examination of tumor markers also provides a basis for diagnosis. Elevated CA199 levels are often seen in mucinous ovarian cancer, borderline tumors and gastrointestinal metastatic ovarian cancer (29-32), whereas increased CEA levels are common in gastrointestinal metastatic ovarian cancer (33-36). In the present case, the elevation of CA199 supported the diagnosis of metastatic ovarian cancer, while CEA did not show a significant increase. However, these tumor marker tests aid in diagnosis but lack specificity. A definitive diagnosis of ovarian metastatic tumors is more reliant on pathological and immunohistochemical examinations. Negative expression of PAX8 can clearly rule out a primary tumor and support a metastatic origin (37), CK7 and CK20 are important markers for distinguishing ovarian tumors (2), and SATB2 is typically highly expressed in the lower epithelial tissues of the gastrointestinal tract (38). In the present case, SATB2 exhibited negative expression.

At present, there is a lack of standards or consensus on the treatment of metastatic ovarian cancer due to an insufficient number of case studies (3,5). While appropriate surgical intervention can prolong the survival time of patients with primary tumors, it is less effective for those with metastatic tumors requiring combined treatment with radiotherapy or chemotherapy, with recurrence often occurring within 2-5 years (39). In the present case, NGS was utilized for genomic analysis of the tumor tissue, revealing mutations at c.4720delC in the *ARID1A* gene and c.35G>C in the *KRAS* gene, with the aim of identifying potential targeted therapies.

ARID1A, also known as *NAA10* (40), is recognized as a tumor suppressor gene that is integral to the SWI/SNF chromatin remodeling complex (41). *ARD1A* has been identified as one of the frequently mutated chromatin remodeling genes in GC (42). Mutations in *ARD1A* across the entire coding region are prevalent in GC, typically resulting in inactivating mutations, including truncating mutations and insertions/deletions that lead to frameshifts (43,44), which have a pivotal role in the initiation, progression and metastasis of cancer, as well as cell cycle arrest (14,18). In terms of pathogenesis, mutations in *ARID1A* can inactivate β-catenin, subsequently reducing the transcription of cyclin D1, leading to cell cycle arrest at the G_0/G_1 phase (18). Although cell cycle arrest is generally considered an anticancer mechanism, certain studies have proposed the concept of the DNA damage model, where cell cycle arrest can, in some cases, drive cells into senescence, increasing the risk of genetic mutations and thereby promoting cancer development (45-47). This suggests that cell cycle arrest induced by *ARID1A* mutations can exert stress on cells, leading to the accumulation of DNA damage and further genetic mutations, thus promoting cancer development.

Previous studies have underscored the importance of *ARID1A* mutations in a spectrum of cancer types, including GC and CRC (14-17); however, their role in metastatic ovarian cancer, such as in Krukenberg tumors, remains inadequately explored. In murine models, *ARD1A* has been demonstrated to stabilize nuclear factor erythroid 2-related factor 2 through direct interaction, thereby promoting the progression of CRC (48). Furthermore, research has established an association between *ARID1A* mutations and OS in patients with GC. In a cohort of 518 patients with GC, immunohistochemical assessments revealed that, compared with those without *ARID1A* mutations, patients with *ARID1A*-mutated GC were older, exhibited higher tumor MSI and had a greater prevalence of *PI3K/AKT* pathway mutations. Multivariate analysis indicated that *ARID1A* mutations were an independent prognostic factor for diffuse-type GC (49). These findings align with the present case, suggesting that *ARID1A* mutations are not isolated events and may have a role in the pathogenesis of Krukenberg tumors. However, large-scale studies specifically targeting Krukenberg tumors are lacking, underscoring the need for further research to substantiate these observations.

In terms of treatment, certain clinical trials of immune checkpoint inhibitors (ICIs) have revealed that *ARID1A* mutations are significantly enriched in responders to immunotherapy across various solid tumor types, independent of MSI (50-54). Patients with *ARID1A*-mutated gastrointestinal tumors have been shown to exhibit more favorable treatment responses to programmed cell death protein 1 (PD-1)/programmed death-ligand 1 (PD-L1) therapies and have improved survival outcomes compared with those with *ARID1A* wild-type tumors (55). Preclinical studies using mouse models have confirmed that the loss of *ARID1A* in tumor cells induces R-loops, and the cellular membrane DNA species produced by R-loops activate the STING/type I IFN signaling pathway, inducing an *ARID1A-IFN* gene expression signature that promotes antitumor immunity (14,19,20), explaining the enhanced responsiveness of *ARID1A*-mutated human tumors to ICIs. ICI therapy has also demonstrated favorable response rates in a multitude of clinical trials involving GC. Interim results from the Phase III MATTERHORN trial have

indicated that the application of a PD-L1 monoclonal antibody (durvalumab) in combination with the FLOT regimen (docetaxel, 5-FU, leucovorin and oxaliplatin) in patients with resectable GC and gastroesophageal junction adenocarcinoma (GEJAC) yields a higher rate of pathological complete response compared with the placebo group (19 vs. 7%) (56). Similarly, preliminary results from the DANTE trial have suggested that the combination of a PD-1 inhibitor (atezolizumab) with chemotherapy is associated with improved safety and efficacy compared with the FLOT regimen alone in patients with resectable GEJAC (57). These clinical data on immunotherapy for GC indicate that ICIs, particularly PD-1 inhibitors, may exhibit promising efficacy and safety profiles for patients with Krukenberg tumors harboring *ARID1A* mutations.

KRAS gene mutations are closely associated with tumor development, and the encoded protein is a key component of the MAPK/ERK signaling pathway (10,11), which can directly promote cell metabolism and proliferation, participate in tumor immune evasion and modulate the immune system response to tumor cells, thereby affecting the tumor microenvironment (12). In the present case, DNA sequencing revealed a *KRAS* mutation corresponding to the amino acid change, p.G12A (glycine at the 12th position), located in a key structural domain of the protein and a known mutation hotspot (58,59). Mutations at G12 affect the binding of KRAS protein to the GTP/GDP cycle, leading to continuous activation of the KRAS protein, abnormal activation of the MAPK/ERK signaling pathway, uncontrolled cell proliferation and ultimately contributes to tumor invasion and metastasis (60-62). *KRAS* mutations are among the most extensively studied and are distinctively characterized oncogenic alterations, occurring in 17-25% of all cancers, with a prevalence of ~9% in GC and 30-40% in CRC (63,64). In a cohort analysis of 595 patients with GC, those with *KRAS* mutations and an MSI status exhibited a longer survival time compared with patients without *KRAS* mutations and a microsatellite stable status (65). Furthermore, *KRAS* harboring the G12 mutation is associated with poorer patient survival in GC (66,67). Warneke *et al* (67) evaluated the prognostic significance of different phenotypic and genotypic markers, including *KRAS*, *PIK3CA* and MSI, in GC and predicted the feasibility of applying these markers in personalized therapy for GC. The results indicated that patients with proximal GC harboring *KRAS* mutations had shorter survival times than those without mutations (3.5 vs. 12.7 months). Additionally, in a study of SRCC of the stomach, immunohistochemistry revealed positive KRAS expression in the majority of SRCC samples, which was higher than in the intestinal-type cohort (28 vs. 12.6%). Concurrently, patients with *KRAS* mutations had a median OS time of 12.5 months, compared with 19.5 months for those without *KRAS* mutations, demonstrating a notable reduction in OS (66).

In the therapeutic domain, studies have confirmed that $KRAS^{G12C}$ inhibitors, such as sotorasib and adagrasib, have shown clinical activity in clinical trials for $KRAS^{G12C}$-mutated non-small cell lung cancer (NSCLC) and CRC (60,61,68,69). Specifically, in patients with NSCLC, a confirmed response rate of 53.4% was observed, with a median progression-free survival (PFS) time of 13.1 months. In CRC, 29.1% of patients exhibited a response, with a PFS time of 5.6 months. Although treatment-related adverse events occurred in 93% of patients, the most common being nausea (74%), diarrhea (61%) and vomiting (58%), the majority were grade 1-2 (94%) and resolved following symptomatic management and drug discontinuation (68). Overall, based on the current clinical data, $KRAS^{G12C}$ inhibitors demonstrate a favorable safety profile in other malignancies, providing preliminary support for their potential application in Krukenberg tumors.

While the present study underscores potential therapeutic strategies based on *ARID1A* mutations and $KRAS^{G12C}$ inhibitors, their clinical application in Krukenberg tumors remains speculative. The rarity of this disease contributes to a scarcity of therapeutic references and research. Considering the unique tumor microenvironment and immune characteristics of Krukenberg tumors, larger cohort studies are necessary to further evaluate the efficacy and safety of immunotherapy in this tumor type.

In conclusion, the present study describes the case of a patient with Krukenberg tumors harboring two mutated genes, and discusses the molecular mechanisms and clinical significance of tumor invasion caused by *ARID1A* and *KRAS* mutations. The mutation in the *ARID1A* gene may increase sensitivity to ICI therapy, whereas the successful application of $KRAS^{G12C}$ inhibitors in other cancer types provides novel insights for targeted therapy of Krukenberg tumors. The patient in the present case achieved an OS time of 30 months from the initial diagnosis of GC, but only 4 months following the recurrence of Krukenberg tumors. This highlights the poor prognosis of this disease and the urgent need for the development of effective therapeutic strategies. Nevertheless, as the first study, to the best of our knowledge, to explore the genomic alterations of Krukenberg tumors, it offers novel insights into the molecular mechanisms of this rare disease. These preliminary findings may stimulate further research to validate the efficacy of these molecular targets, ultimately improving patient treatment outcomes.

Acknowledgements

The authors would like to thank Dr Feng Na (Department of Pathology, Dongguan Songshan Lake Hospital, Dongguan, China) for the assistance and expertise contributed to the present study.

Funding

This study was supported by a grant from the Dongguan Social Development and Technology Program (grant no. 20211800901802).

Availability of data and materials

The datasets generated in the present study may be found in the NCBI database under accession number PRJNA1240087 or at the following URL: https://www.ncbi.nlm.nih.gov/sra/?term=PRJNA1240087.

Authors' contributions

JW was responsible for the conception and design of the study, and drafted the manuscript. Data collection and analysis

were carried out by JW, SJ and QS. JW and HG confirm the authenticity of all the raw data. HG contributed to the study design and participated in the interpretation of the results. The entire study was supervised by HG. All authors have read and approved the final version of the manuscript.

Ethics approval and consent to participate

The present study was carried out in accordance with institutional guidelines and was approved by the Ethics Committee of Dongguan Songshan Lake Tungwah Hospital (Dongguan, China; approval no. SDHKY-2024-008-01), as it involved detailed clinical features and sequencing data analysis beyond standard case reporting. The study was conducted in accordance with institutional guidelines and The Declaration of Helsinki. Written informed consent was obtained from the patient for participation.

Patient consent for publication

The patient provided written informed consent for the publication of the present case report.

Competing interests

The authors declare that they have no competing interests.

References

1. Kossai M, Leary A, Scoazec JY and Genestie C: Ovarian cancer: A heterogeneous disease. Pathobiology 85: 41-49, 2018.
2. Al-Agha OM and Nicastri AD: An in-depth look at Krukenberg tumor an overview. Arch Pathol Lab Med 130: 1725-1730, 2006.
3. Kiyokawa T, Young RH and Scully RE: Krukenberg tumors of the ovary a clinicopathologic analysis of 120 cases with emphasis on their variable pathologic manifestations. Am J Surg Pathol 30: 277-299, 2006.
4. Yada-Hashimoto N, Yamamoto T, Kamiura S, Seino H, Ohira H, Sawai K, Kimura T and Saji F: Metastatic ovarian tumors: A review of 64 cases. Gynecol Oncol 89: 314-317, 2003.
5. Kodama M, Moeini A, Machida H, Blake EA, Grubbs BH and Matsuo K: Feto-maternal outcomes of pregnancy complicated by Krukenberg tumor: A systematic review of literature. Arch Gynecol Obstet 294: 589-598, 2016.
6. Wang B, Tang Q, Xu L, Teng X, Ding W, Ren G and Wang X: A comparative study of RTK gene status between primary tumors, lymph-node metastases, and Krukenberg tumors. Mod Pathol 34: 42-50, 2021.
7. Timar J and Kashofer K: Molecular epidemiology and diagnostics of KRAS mutations in human cancer. Cancer Metastasis Rev 39: 1029-1038, 2020.
8. Prior IA, Hood FE and Hartley JL: The frequency of ras mutations in cancer. Cancer Res 80: 2969-2974, 2020.
9. Cook JH, Melloni GEM, Gulhan DC, Park PJ and Haigis KM: The origins and genetic interactions of KRAS mutations are allele- and tissue-specific. Nat Commun 12: 1808, 2021.
10. Cox AD, Fesik SW, Kimmelman AC, Luo J and Der CJ: Drugging the undruggable RAS: Mission possible? Nat Rev Drug Discov 13: 828-851, 2014.
11. Downward J: Targeting RAS signalling pathways in cancer therapy. Nat Rev Cancer 3: 11-22, 2003.
12. Hsu WH, LaBella KA, Lin Y, Xu P, Lee R, Hsieh CE, Yang L, Zhou A, Blecher JM, Wu CJ, *et al*: Oncogenic KRAS drives lipofibrogenesis to promote angiogenesis and colon cancer progression. Cancer Discov 13: 2652-2673, 2023.
13. Lee D, Jang MK, Seo JH, Ryu SH, Kim JA and Chung YH: ARD1/NAA10 in hepatocellular carcinoma: Pathways and clinical implications. Exp Mol Med 50: 1-12, 2018.
14. Vokshi BH and Toska E: Mutant ARID1A: Igniting cancer immunotherapy. Trends Immunol 45: 565-567, 2024.
15. Mullen J, Kato S, Sicklick JK and Kurzrock R: Targeting ARID1A mutations in cancer. Cancer Treat Rev 100: 102287, 2021.
16. Takeda T, Banno K, Okawa R, Yanokura M, Iijima M, Irie-Kunitomi H, Nakamura K, Iida M, Adachi M, Umene K, *et al*: ARID1A gene mutation in ovarian and endometrial cancers (Review). Oncol Rep 35: 607-613, 2016.
17. Fontana B, Gallerani G, Salamon I, Pace I, Roncarati R and Ferracin M: ARID1A in cancer: Friend or foe? Front Oncol 13: 1136248, 2023.
18. Lim JH, Park JW and Chun YS: Human arrest defective 1 acetylates and activates beta-catenin, promoting lung cancer cell proliferation. Cancer Res 66: 10677-10682, 2006.
19. Maxwell MB, Hom-Tedla MS, Yi J, Li S, Rivera SA, Yu J, Burns MJ, McRae HM, Stevenson BT, Coakley KE, *et al*: ARID1A suppresses R-loop-mediated STING-type I interferon pathway activation of anti-tumor immunity. Cell 187: 3390-3408.e3319, 2024.
20. Goswami S and Sharma P: Loss of ARID1A 'loops' in STING. Trends Immunol 45: 568-570, 2024.
21. Berek JS, Renz M, Kehoe S, Kumar L and Friedlander M: Cancer of the ovary, fallopian tube, and peritoneum: 2021 update. Int J Gynaecol Obstet 155 (Suppl 1): S61-S85, 2021.
22. Classic pages in obstetrics and gynecology: Friedrich Ernst Krukenberg: Fibrosarcoma ovarii mucocellulare (carcinomatodes). Archiv für Gynäkologie, vol 50, pp. 287-321, 1896. Am J Obstet Gynecol 117: 575, 1973.
23. Kubeček O, Laco J, Špaček J, Petera J, Kopecký J, Kubečková A and Filip S: The pathogenesis, diagnosis, and management of metastatic tumors to the ovary: A comprehensive review. Clin Exp Metastasis 34: 295-307, 2017.
24. Zhou Z, Li C, Wang Z, Haybaeck J and Zhang C: Cd44v6 acts as a directional responding factor in the process of transcoelomic metastasis from gastric carcinoma to Krukenberg tumor. Expert Rev Mol Diagn 23: 583-588, 2023.
25. Thakur P, Sharma M, Chauhan A, Pal KM, Thakur S, Gupta M and Kaushal S: Colorectal origin: A marker of favorable outcome in Krukenberg Tumor? Results from Clinical and Prognostic Analysis. South Asian J Cancer 13: 99-105, 2024.
26. Wu F, Zhao X, Mi B, Feng LU, Yuan NA, Lei F, Li M and Zhao X: Clinical characteristics and prognostic analysis of Krukenberg tumor. Mol Clin Oncol 3: 1323-1328, 2015.
27. Scully RE and Sobin LH: Histologic typing of ovarian tumors. Arch Pathol Lab Med 111: 794-795, 1987.
28. Karaosmanoglu AD, Onur MR, Salman MC, Usubutun A, Karcaaltincaba M, Ozmen MN and Akata D: Imaging in secondary tumors of the ovary. Abdom Radiol (NY) 44: 1493-1505, 2019.
29. Zhang M, Shi M, Yu Y, Sang J, Wang H, Shi J, Duan P and Ge R: The immune subtypes and landscape of advanced-stage ovarian cancer. Vaccines (Basel) 10: 1451, 2022.
30. Guo J, Yu J, Song X and Mi H: Serum CA125, CA199 and CEA combined detection for epithelial ovarian cancer diagnosis: A meta-analysis. Open Med (Wars) 12: 131-137, 2017.
31. Wang Y, Liu L and Yu Y: Mucins and mucinous ovarian carcinoma: Development, differential diagnosis, and treatment. Heliyon 9: e19221, 2023.
32. Matsas A, Stefanoudakis D, Troupis T, Kontzoglou K, Eleftheriades M, Christopoulos P, Panoskaltsis T, Stamoula E and Iliopoulos DC: Tumor markers and their diagnostic significance in ovarian cancer. Life (Basel) 13: 1689, 2023.
33. Hu J, Khalifa RD, Roma AA and Fadare O: The pathologic distinction of primary and metastatic mucinous tumors involving the ovary: A re-evaluation of algorithms based on gross features. Ann Diagn Pathol 37: 1-6, 2018.
34. Hall C, Clarke L, Pal A, Buchwald P, Eglinton T, Wakeman C and Frizelle F: A review of the role of carcinoembryonic antigen in clinical practice. Ann Coloproctol 35: 294-305, 2019.
35. Locker GY, Hamilton S, Harris J, Jessup JM, Kemeny N, Macdonald JS, Somerfield MR, Hayes DF and Bast RC Jr; ASCO: ASCO 2006 update of recommendations for the use of tumor markers in gastrointestinal cancer. J Clin Oncol 24: 5313-5327, 2006.
36. Sturgeon CM, Duffy MJ, Stenman UH, Lilja H, Brünner N, Chan DW, Babaian R, Bast RC Jr, Dowell B, Esteva FJ, *et al*: National Academy of clinical biochemistry laboratory medicine practice guidelines for use of tumor markers in testicular, prostate, colorectal, breast, and ovarian cancers. Clin Chem 54: e11-e79, 2008.
37. Ozcan A, Shen SS, Hamilton C, Anjana K, Coffey D, Krishnan B and Truong LD: PAX 8 expression in non-neoplastic tissues, primary tumors, and metastatic tumors: A comprehensive immunohistochemical study. Mod Pathol 24: 751-764, 2011.

38. Berg KB and Schaeffer DF: SATB2 as an immunohistochemical marker for colorectal adenocarcinoma: A concise review of benefits and pitfalls. Arch Pathol Lab Med 141: 1428-1433, 2017.
39. Kuroki L and Guntupalli SR: Treatment of epithelial ovarian cancer. BMJ 371: m3773, 2020.
40. Kuhns KJ, Zhang G, Wang Z and Liu W: ARD1/NAA10 acetylation in prostate cancer. Exp Mol Med 50: 1-8, 2018.
41. Wu RC, Wang TL and Shih IM: The emerging roles of ARID1A in tumor suppression. Cancer Biol Ther 15: 655-664, 2014.
42. Chia NY and Tan P: Molecular classification of gastric cancer. Ann Oncol 27: 763-769, 2016.
43. Zang ZJ, Cutcutache I, Poon SL, Zhang SL, McPherson JR, Tao J, Rajasegaran V, Heng HL, Deng N, Gan A, *et al*: Exome sequencing of gastric adenocarcinoma identifies recurrent somatic mutations in cell adhesion and chromatin remodeling genes. Nat Genet 44: 570-574, 2012.
44. Wang K, Kan J, Yuen ST, Shi ST, Chu KM, Law S, Chan TL, Kan Z, Chan AS, Tsui WY, *et al*: Exome sequencing identifies frequent mutation of ARID1A in molecular subtypes of gastric cancer. Nat Genet 43: 1219-1223, 2011.
45. Halazonetis TD, Gorgoulis VG and Bartek J: An oncogene-induced DNA damage model for cancer development. Science 319: 1352-1355, 2008.
46. Vogelstein B and Kinzler KW: Cancer genes and the pathways they control. Nat Med 10: 789-799, 2004.
47. Xue W, Zender L, Miething C, Dickins RA, Hernando E, Krizhanovsky V, Cordon-Cardo C and Lowe SW: Senescence and tumour clearance is triggered by p53 restoration in murine liver carcinomas. Nature 445: 656-660, 2007.
48. Fang X, Lee YH, Jang JH, Kim SJ, Kim SH, Kim DH, Na HK, Kim KO, Baek JH and Surh YJ: ARD1 stabilizes NRF2 through direct interaction and promotes colon cancer progression. Life Sci 313: 121217, 2023.
49. Wu CH, Tseng CH, Huang KH, Fang WL, Chen MH, Li AFY and Wu CW: The clinical signiicance of ARID1A mutations in gastric cancer patients. Formosan J Surg 53: 93-100, 2020.
50. Okamura R, Kato S, Lee S, Jimenez RE, Sicklick JK and Kurzrock R: ARID1A alterations function as a biomarker for longer progression-free survival after anti-PD-1/PD-L1 immunotherapy. J Immunother Cancer 8: e000438, 2020.
51. Botta GP, Kato S, Patel H, Fanta P, Lee S, Okamura R and Kurzrock R: SWI/SNF complex alterations as a biomarker of immunotherapy efficacy in pancreatic cancer. JCI Insight 6: e150453, 2021.
52. Goswami S, Chen Y, Anandhan S, Szabo PM, Basu S, Blando JM, Liu W, Zhang J, Natarajan SM, Xiong L, *et al*: ARID1A mutation plus CXCL13 expression act as combinatorial biomarkers to predict responses to immune checkpoint therapy in mUCC. Sci Transl Med 12: eabc4220, 2020.
53. Li L, Li M, Jiang Z and Wang X: ARID1A mutations are associated with increased immune activity in gastrointestinal cancer. Cells 8: 678, 2019.
54. Wang FH, Wei XL, Feng J, Li Q, Xu N, Hu XC, Liao W, Jiang Y, Lin XY, Zhang QY, *et al*: Efficacy, safety, and correlative biomarkers of toripalimab in previously treated recurrent or metastatic nasopharyngeal carcinoma: A phase II clinical trial (POLARIS-02). J Clin Oncol 39: 704-712, 2021.
55. Gu Y, Zhang P, Wang J, Lin C, Liu H, Li H, He H, Li R, Zhang H and Zhang W: Somatic ARID1A mutation stratifies patients with gastric cancer to PD-1 blockade and adjuvant chemotherapy. Cancer Immunol Immunother 72: 1199-1208, 2023.
56. Janjigian YY, Al-Batran SE, Wainberg ZA, Cutsem EV, Molena D, Muro K, Hyung WJ, Wyrwicz LS, Oh DY, Omori T, *et al*: Pathological complete response (pCR) to 5-fluorouracil, leucovorin, oxaliplatin and docetaxel (FLOT) with or without durvalumab (D) in resectable gastric and gastroesophageal junction cancer (GC/GEJC): Subgroup analysis by region from the phase 3, randomized, double-blind MATTERHORN study. J Clin Oncol 42: LBA246-LBA246, 2024.
57. Lorenzen S, Götze TO, Thuss-Patience P, Biebl M, Homann N, Schenk M, Lindig U, Heuer V, Kretzschmar A, Goekkurt E, *et al*: Perioperative atezolizumab plus fluorouracil, leucovorin, oxaliplatin, and docetaxel for resectable esophagogastric cancer: Interim results from the randomized, multicenter, phase II/III DANTE/IKF-s633 trial. J Clin Oncol 42: 410-420, 2023.
58. Prior IA, Lewis PD and Mattos C: A comprehensive survey of Ras mutations in cancer. Cancer Res 72: 2457-2467, 2012.
59. Forbes SA, Bindal N, Bamford S, Cole C, Kok CY, Beare D, Jia M, Shepherd R, Leung K, Menzies A, *et al*: COSMIC: Mining complete cancer genomes in the catalogue of somatic mutations in cancer. Nucleic Acids Res 39: D945-D950, 2011.
60. Reck M, Carbone DP, Garassino M and Barlesi F: Targeting KRAS in non-small-cell lung cancer: Recent progress and new approaches. Ann Oncol 32: 1101-1110, 2021.
61. Melosky B, Wheatley-Price P, Juergens RA, Sacher A, Leighl NB, Tsao MS, Cheema P, Snow S, Liu G, Card PB and Chu Q: The rapidly evolving landscape of novel targeted therapies in advanced non-small cell lung cancer. Lung Cancer 160: 136-151, 2021.
62. Scheffzek K, Ahmadian MR, Kabsch W, Wiesmüller L, Lautwein A, Schmitz F and Wittinghofer A: The Ras-RasGAP complex: Structural basis for GTPase activation and its loss in oncogenic Ras mutants. Science 277: 333-338, 1997.
63. Cancer Genome Atlas Research Network: Comprehensive molecular characterization of gastric adenocarcinoma. Nature 513: 202-209, 2014.
64. Arrington AK, Heinrich EL, Lee W, Duldulao M, Patel S, Sanchez J, Garcia-Aguilar J and Kim J: Prognostic and predictive roles of KRAS mutation in colorectal cancer. Int J Mol Sci 13: 12153-12168, 2012.
65. Polom K, Das K, Marrelli D, Roviello G, Pascale V, Voglino C, Rho H, Tan P and Roviello F: KRAS Mutation in gastric cancer and prognostication associated with microsatellite instability status. Pathol Oncol Res 25: 333-340, 2019.
66. Wu N, Huang Y, Liu F, Xu X, Liu B and Wei J: KRAS gene status in gastric signet-ring cell carcinoma patients and acts as biomarker of MEK inhibitor. J Gastrointest Oncol 12: 1020-1030, 2021.
67. Warneke VS, Behrens HM, Haag J, Balschun K, Böger C, Becker T, Ebert MP, Lordick F and Röcken C: Prognostic and putative predictive biomarkers of gastric cancer for personalized medicine. Diagn Mol Pathol 22: 127-137, 2013.
68. Sacher A, LoRusso P, Patel MR, Miller WH Jr, Garralda E, Forster MD, Santoro A, Falcon A, Kim TW, Paz-Ares L, *et al*: Single-Agent Divarasib (GDC-6036) in solid tumors with a KRAS G12C mutation. N Engl J Med 389: 710-721, 2023.
69. Canon J, Rex K, Saiki AY, Mohr C, Cooke K, Bagal D, Gaida K, Holt T, Knutson CG, Koppada N, *et al*: The clinical KRAS(G12C) inhibitor AMG 510 drives anti-tumour immunity. Nature 575: 217-223, 2019.